Environ. Sci. Technol. **2005**, *39,* 1250−1256

Using a Surface Complexation Model To Predict the Nature and Stability of Nanoparticles

KEISUKE FUKUSHI[†,‡] AND
TSUTOMU SATO[*,§]

Research Center for Deep Geological Environments, National Institute of Advanced Industrial Science and Technology (AIST), Tsukuba, Ibaraki 305-8567, Japan, and Institute of Nature & Environmental Technology, Kanazawa University, Kanazawa, Ishikawa 920-1192, Japan

Nanoparticles are discrete nanometer-scale assemblies of atoms and have dimensions between those characteristic of ions and those of macroscopic materials. These minerals commonly possess extremely large specific surface areas and surface adsorption capacities for foreign ions. Due to the large specific surface area and large fraction of surface atoms, the natures of nanoparticles are expected to be modified by the adsorption (surface complexation) process. In this paper, we discuss theoretically the stability of nanoparticles that make the surface complex with foreign ions. The principal theoretical assumption is that the surface complexation occurs at the bulk of the nanoparticles, as in a solid solution. The surface complexation affects two aspects of the intrinsic stability of the nanoparticles simultaneously: one is the composition of the nanoparticles; the other is the free energy of formation of nanoparticles. The solubility of hydrous ferric oxide (HFO) was estimated by using surface complexation modeling coupled with published data of the free energy of formation of the relevant components. The solubility modeling of surface-charged (H^+ or OH^- sorbed) HFO mechanistically and quantitatively explained the observed nonintegral behavior of the solubility of HFO. Moreover, solubility modeling of anion (SO_4^{2-}, PO_4^{3-}, and As(V)) sorption by HFO showed that the sorption process strongly influences the stability of the nanoparticles. This result implies that geochemical modeling leads to the erroneous prediction of a natural system if the effect of the sorption process is not taken into account.

Introduction

Nanoparticles are discrete nanometer (10^{-9} m) scale assemblies of atoms and have dimensions between those characteristic of ions (10^{-10} m) and those of macroscopic materials (*1*). Iron oxides (hydrous ferric oxide, schwertmannite, and goethite), aluminum hydroxide (gibbsite, amorphous aluminum hydroxide), and aluminum silicate minerals (allophane and imogorite) are commonly encountered nanoparticles in the surface and subsurface environment. These minerals commonly possess extremely large specific surface areas and surface adsorption capacities for foreign ions (*1*). The structure of the surface on a nanoparticle may be essentially indistinguishable from the structure of the equivalent surface on a macroscopic crystal. However, a significant fraction of the atoms are exposed on the surface rather than contained in the bulk (*1*). Therefore, the natures of nanoparticles are expected to be modified by the adsorption (surface complexation) process (*2*, *3*).

Several studies have indicated that, under acidic to neutral pH conditions, precipitates of hydrous ferric oxide (HFO) formed and aged at low temperature, exhibit solubility products of the form $K_{SO} = a_{Fe^{3+}} a_{H^+}{}^{-m}$, where $m < 3$ (e.g., see Figure 1) (*4*−*6*). Biedermann and Chow (*4*) and Fox (*5*) indicated that charge-neutral precipitates were obtained through incorporation of counterions in the matrix of the HFO precipitates. The postulated solid phases were $Fe(OH)_{3-n}(A)_n$, where A was Cl, NO_3, or ClO_4. Because the mass action law for the dissolution reaction can be described as $K'_{SO} = a_{Fe^{3+}} a_{H^+}{}^{-(3-n)}$, the m in $K_{SO} = a_{Fe^{3+}} a_{H^+}{}^{-m}$ must be less than 3. Although Biedermann and Chow (*4*) and Fox (*5*) took into account the effects of anion incorporation to explain the nonintegral behavior of HFO solubility, they did not consider the mechanisms and behaviors of anion incorporation. Anion incorporation in HFO may be explained within the framework of the surface complexation theory (*7*−*9*). Counterions such as Cl^-, NO_3^-, or ClO_4^- electrostatically adsorb to the protonated surface hydroxyl (denoted $\equiv FeOH_2^+$) (or make outer-sphere surface complexes) as follows:

$$\equiv FeOH_2^+ + A^- \rightarrow \equiv FeOH_2^+ : A^- \qquad (1)$$

where ":" denotes water molecules. When the chemical composition of ideal HFO is assumed to be $Fe(OH)_3$, the number of moles of surface hydroxyl groups per mole of HFO is calculated to be 0.2 mol/mol (*7*). If the surface hydroxyl groups of HFO are wholly protonated under acidic conditions, the HFO contains 0.2 mol of monovalent counterions such as Cl^-, NO_3^-, or ClO_4^- in order to neutralize the surface charge. Although the anion content varies with solution conditions such as pH and ionic strength (*7*−*9*), under acidic conditions, the n in $Fe(OH)_{3-n}$ must take a positive value under the condition of which pH is less than the point of zero charge of HFO. This example shows that surface complexations lead to changes in chemical composition, which further lead to changes in the intrinsic stability of the nanoparticles.

Sorption processes influence the stability as exemplified above. However, the theoretical aspects of these processes have not yet been considered. To understand the nature of nanoparticles, it is important to consider the effect of surface complexation on the stability of nanoparticles. Moreover, quantitative prediction of the stability of nanoparticles that make the surface complexation is important in modeling their fate and the behavior of dissolved elements sorbed to nanoparticles in surface and subsurface environments. In this paper, we demonstrate that geochemical parameters such as the free energy of formation and surface complexation constants can be used to predict the stability of nanoparticles and that the nature of nanoparticles strongly depends on the surface complexation process.

Theoretical Development

The principal theoretical assumption is that the surface complexation occurs at the bulk of the nanoparticles, as in a solid solution. With this assumption, the surface exists throughout the bulk of the nanoparticles. In studies of

---

[*] Corresponding author phone: +81-76-264-5725; fax: +81-76-264-5746; e-mail: tomsato@earth.s.kanazawa-u.ac.jp.

[†] AIST.

[‡] Present address: Department of Earth and Planetary Sciences, Johns Hopkins University, Baltimore, MD 21218.

[§] Kanazawa University.

10.1021/es0491984 CCC: $30.25

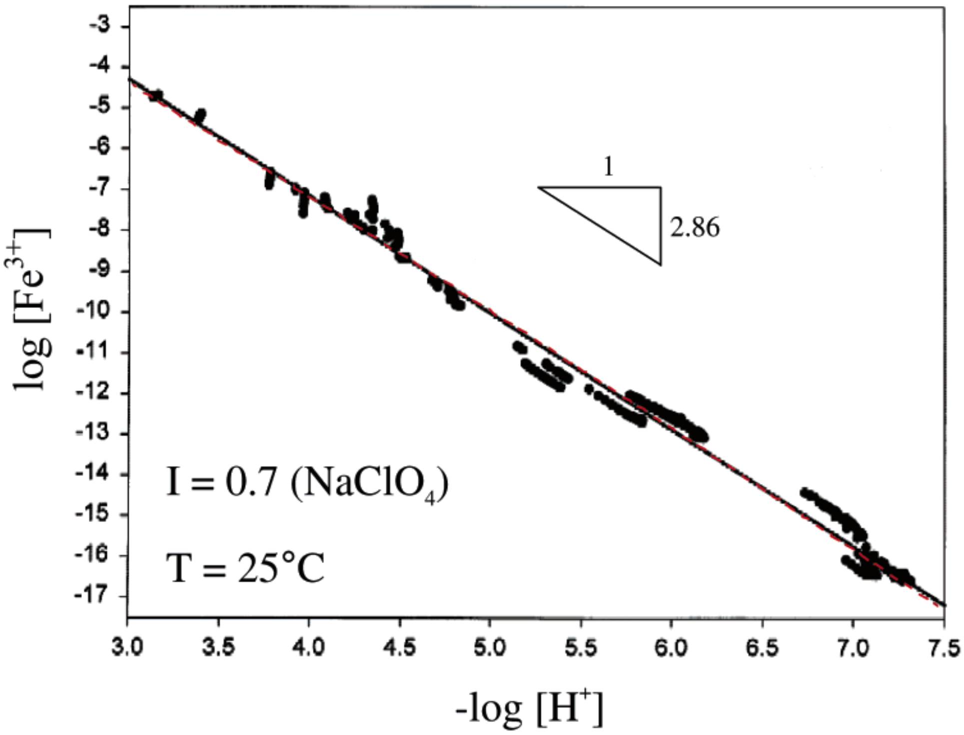

FIGURE 1. Relationship between log[Fe^{3+}] and $-$log[H$^+$] in 0.7 M NaClO$_4$ at 25 °C (modified from Byrne and Luo; 6). The solid black line shows the linear regression of observed data (log[Fe^{3+}] $= 4.28 + 2.86$ log[H$^+$]). The dotted red line shows the results of theoretical calculation assuming ΔG_f^0(HFO) $= -693$ kJ/mol.

arsenate sorption onto schwertmannite, Fukushi et al. (*2*, *10*) demonstrated that the mechanism of As(V) sorption was identical to surface ligand exchange with the surface sulfate group of schwertmannite and that the exchange reaction could quantitatively be expressed as an ideal solid−solution reaction. Our observations support the validity of this assumption. Surface complexation affects two aspects of the intrinsic stability of nanoparticles simultaneously: one is the composition of the nanoparticles; the other is the free energy of formation of nanoparticles. For simplicity, we first construct the theory with protonation and deprotonation of surface hydroxyl groups of trivalent metal trihydroxide (Me(OH)$_3$). Using the simple 2p*K* one-site model, we write the surface protonation and deprotonation reactions of Me(OH)$_3$ as

$$\equiv\mathrm{MeOH} + \mathrm{H}^+ = \equiv\mathrm{MeOH_2}^+ \quad K_{\mathrm{prot}} \tag{2}$$

$$\equiv\mathrm{MeOH} = \equiv\mathrm{MeO}^- + \mathrm{H}^+ \quad K_{\mathrm{deprot}} \tag{3}$$

where $\equiv$MeOH, $\equiv$MeOH$_2^+$, and $\equiv$MeO$^-$ denote neutral, positively charged, and negatively charged surface hydroxyl groups, respectively, and K_{prot} and K_{deprot} are the total (or apparent) protonation and deprotonation constants of surface hydroxyl groups. The free energy change with sorption of 1 mol of H$^+$ ($\Delta G_R^{\mathrm{prot}}$) is

$$\Delta G_R^{\mathrm{prot}} = -2.303RT \log K_{\mathrm{prot}} \tag{4}$$

, and the free energy change with desorption of 1 mol of H$^+$ ($\Delta G_R^{\mathrm{deprot}}$) is

$$\Delta G_R^{\mathrm{deprot}} = -2.303RT \log K_{\mathrm{deprot}} \tag{5}$$

where *R* and *T* denote the ideal gas constant and the absolute temperature. The free energy changes ($\Delta G_R^{\mathrm{prot}}$ and $\Delta G_R^{\mathrm{deprot}}$) contain both the free energy change of chemical (intrinsic) force and the free energy change of Coulombic force (*7*−*9*).The change in bulk composition of Me(OH)$_3$ by protonation and deprotonation can be written as

$$\mathrm{Me(OH)_3} + x\mathrm{H}^+ = \mathrm{Me(OH)}_{3-x}{}^{x} + x\mathrm{H_2O} \tag{6}$$

$$\mathrm{Me(OH)_3} + y\mathrm{H_2O} = \mathrm{Me(OH)}_{3+y}{}^{-y} + y\mathrm{H}^+ \tag{7}$$

where *x* and *y* denote the moles of H$^+$ sorbed to and desorbed from Me(OH)$_3$, respectively. Reactions 6 and 7 would occur simultaneously; thus, the overall reaction should be written as

$$\mathrm{Me(OH)_3} + x\mathrm{H}^+ + y\mathrm{H_2O} = \mathrm{Me(OH)}_{3-x+y}{}^{x-y} + x\mathrm{H_2O} + y\mathrm{H}^+ \tag{8}$$

The free energy change with reaction 8 ($\Delta G_R^{\mathrm{bulk}}$) is given as

$$\Delta G_R^{\mathrm{bulk}} = \Delta G_f^0(\mathrm{Me(OH)}_{3-x+y}{}^{x-y}) + (x - \mathrm{y})\Delta G_f^0(\mathrm{H_2O}) + (y - x)\Delta G_f^0(\mathrm{H}^+) - \Delta G_f^0(\mathrm{Me(OH)_3}) \tag{9}$$

Because the work done with *x* moles of protonation (eq 2) and *y* moles of deprotonation (eq 3) would be equivalent to the work done with eqs 6 and 7, respectively, $\Delta G_R^{\mathrm{bulk}}$ can be related to $\Delta G_R^{\mathrm{prot}}$ and $\Delta G_R^{\mathrm{deprot}}$:

$$\Delta G_R^{\mathrm{bulk}} = x\Delta G_R^{\mathrm{prot}} + y\Delta G_R^{\mathrm{deprot}} \tag{10}$$

Therefore, the free energy of formation of Me(OH)$_{3-x+y}{}^{x-y}$ (ΔG_f^0(Me(OH)$_{3-x+y}{}^{x-y}$)), that is, the stability of the charged metal trihydroxide, can be estimated by the following expression:

$$\Delta G_f^0(\mathrm{Me(OH)}_{3-x+y}{}^{x-y}) = x\Delta G_R^{\mathrm{prot}} + y\Delta G_R^{\mathrm{deprot}} - (x - y)\,\Delta G_f^0(\mathrm{H_2O}) - (y - x)\,\Delta G_f^0(\mathrm{H}^+) + \Delta G_f^0(\mathrm{Me(OH)_3}) \tag{11}$$

As indicated in the above equations, the changes in com-

TABLE 1. Surface Complexation Constants and Surface Properties of HFO[a]

reaction	log *K*	source
$\equiv FeOH + H^+ = \equiv FeOH_2^+$	−7.23	*b*
$\equiv FeOH = \equiv FeO^- + H^+$	8.95	*b*
$\equiv FeOH + PO_4^{3-} + 3H^+ = \equiv FeH_2PO_4 + H_2O$	31.29	*b*
$\equiv FeOH + PO_4^{3-} + 2H^+ = \equiv FeHPO_4^- + H_2O$	25.39	*b*
$\equiv FeOH + PO_4^{3-} + H^+ = \equiv FePO_4^{2-} + H_2O$	17.72	*b*
$\equiv FeOH + AsO_4^{3-} + 3H^+ = \equiv FeH_2AsO_4 + H_2O$	29.31	*b*
$\equiv FeOH + AsO_4^{3-} + 2H^+ = \equiv FeHAsO_4^- + H_2O$	23.51	*b*
$\equiv FeOH + AsO_4^{3-} = \equiv FeOHAsO_4$	10.58	*b*
$\equiv FeOH + SO_4^{2-} + H^+ = \equiv FeSO_4^- + H_2O$	7.78	*b*
$\equiv FeOH + SO_4^{2-} = \equiv FeOHSO_4^{2-}$	0.79	*b*
specific surface area:	600 m^2/g	*b*
surface hydroxyl density:	0.2 mol/ mol (HFO)	*b*

[a] Temperature = 25 °C. [b] Ref *12*.

TABLE 2. Free Energies of Formation (ΔG_f^0) of Relevant Components[a]

species	ΔG_f^0 (kJ/mol)	source
Fe^{3+}	−4.6	*b*
HFO ($Fe(OH)_3$)	−699	*b*
H^+	0	*b*
H_2O	−237.18	*b*
PO_4^{3-}	−1018.8	*b*
AsO_4^{3-}	−636	*b*
SO_4^{2-}	−744.6	*b*

[a] Temperature = 25 °C. [b] Ref *14*.

TABLE 3. Association Constantsa of PO_4, As(V), Fe(III), and SO_4

reaction	log *K*	source
$H_3AsO_4(aq) = 3H^+ + AsO_4^-$	−20.60	*b*
$H_2AsO_4^- = 2H^+ + AsO_4^{3-}$	−18.35	*b*
$HAsO_4^{2-} = H^+ + AsO_4^{3-}$	−11.60	*b*
$H_3PO_4(aq) = 3H^+ + PO_4^{3-}$	−21.66	*b*
$H_2PO_4^- = 2H^+ + PO_4^{3-}$	−19.51	*b*
$HPO_4^{2-} = H^+ + PO_4^{3-}$	−12.31	*b*
$HSO_4^- = H^+ + SO_4^{2-}$	−1.99	*b*
$OH^- + H^+ = H_2O$	14.00	*b*
$FeOH_2^+ + H^+ = Fe^{3+} + H_2O$	2.19	*c*
$Fe(OH)_2^+ + 2H^+ = Fe^{3+} + 2H_2O$	5.67	*c*
$Fe(OH)_3(aq) + 3H^+ = Fe^{3+} + 3H_2O$	12.56	*c*
$Fe(OH)_4^- + 4H^+ = Fe^{3+} + 4H_2O$	21.6	*c*

[a] Temperature = 25 °C. [b] Ref *12*. [c] Ref *14*.

position is driven by the work with surface complexation, and the changes in $\Delta G_f^0(Me(OH)_{3-x+y}{}^{x-y})$ are caused by changes in the composition of nanoparticles. Therefore, it is impossible to divide the overall effect to both contributions separately.

The stability of nanoparticles can be estimated by using the free energy of formation of the relevant species and their surface complexation constants. For a more complicated multicomponent solution, a similar procedure can be applied if surface complexation constants are available. On the other hand, there are some limitations on the application of this approach to some kinds of nanoparticles. The present approach assumes that the surface complexation occurs as in an ideal solid−solution and that the mixing of bulk atoms to surface-coordinated atoms is homogeneous. This approach would be valid for the nanoparticles of which ratios of bulk atoms to surface-coordinated atoms and crystallinities are very low. Colloidal nanoparticles such as HFO and amorphous aluminum hydroxide may be smaller and have less crystalline structure than other types of nanoparticles and may be more suitable for this approach. In the case of larger and/or crystalline nanoparticles, the mixing of bulk atoms to surface-coordinated atoms would be heterogeneous depending on the solid-phase properties (such as size and elastic property). To take into account the heterogeneity, this approach should be extended to explain the heterogeneous solid−solution reactions.

Modeling the Stability of Nanoparticles

Effect of Surface Charging. We used HFO as a model material to exemplify the effect of surface complexation on the stability of nanoparticles. HFO is one of the most impotent nanoparticle in surface and subsurface environment (*11*), and the consistent data set for surface complexation modeling is available by using the diffuse layer model (*7*). Surface complexation modeling (SCM) was conducted by using REACT in *The Geochemist's Workbench* (*12*). The intrinsic surface complexation constants, surface site density, and specific surface area were obtained from the FeOH.dat database incorporated in *The Geochemist's Workbench* (based on the compilation by Dzombak and Morel (*7*); Table 1). The free energies of formation of the relevant components are summarized in Table 2. The association constants of the relevant species are summarized in Table 3. $NaClO_4$ was used for inert electrolyte. The activity coefficient was calculated by using extended Debye−Hückel equation (*12*, *13*). The Debye−Hückel b_ν and å parameter is 0.0640 kg/mol and 5.5 Å, respectively for $NaClO_4$ media (*13*). Although we used the diffuse layer model for all calculation because of lack of the consistent data set for other surface complexation models, this approach can be applied for other of surface complexation models. The diffuse layer model cannot take into account the distinctions of both inner- and outer-sphere complexation. The use of other type of surface complexation models that can predict the behavior of the outer-sphere complexes (such as triple layer model) would be appropriate for the accurate prediction when the system contains some ions which make both inner- and outer-sphere complexes.

Figure 2a shows the compositional change of HFO as a function of pH and ionic strength. The composition of HFO was calculated according to eqs 6 and 7. The composition of HFO depends on ionic strength, because the ionic strength strongly influences the protonation/deprotonation behavior (*7*). Figure 2b shows the changes in total (apparent) protonation and deprotonation constants of the surface hydroxyl groups. The constants were directly evaluated by using the calculated concentrations of the surface species as a function of pH and ionic strength:

$$\log K_{prot} = \log[\equiv FeOH_2^+] - \log[\equiv FeOH] + pH \quad (12)$$

$$\log K_{deprot} = \log[\equiv FeO^-] - \log[\equiv FeOH] - pH \quad (13)$$

The variability of the constants is due to the effect of the Coulombic force, which is calculated by the diffuse layer model in REACT. Figure 2c shows the changes in $\Delta G_f(Fe(OH)_{3-x+y}{}^{x-y})$ calculated according to eq 11 as a function of pH and ionic strength. The dissolution reaction of HFO is given as

$$Fe(OH)_{3-x+y}{}^{x-y} + (3 - x + y)H^+ = Fe^{3+} + (3 - x + y)H_2O \quad (14)$$

The free energy change of the reaction (ΔG_R^{dis}) is

$$\Delta G_R^{dis} = \Delta G_f^0(Fe^{3+}) + (3 - x + y)\Delta G_f^0(H_2O) - (3 - x + y)\Delta G_f^0(H^+) - \Delta G_f^0(Fe(OH)_{3-x+y}{}^{x-y}) \quad (15)$$

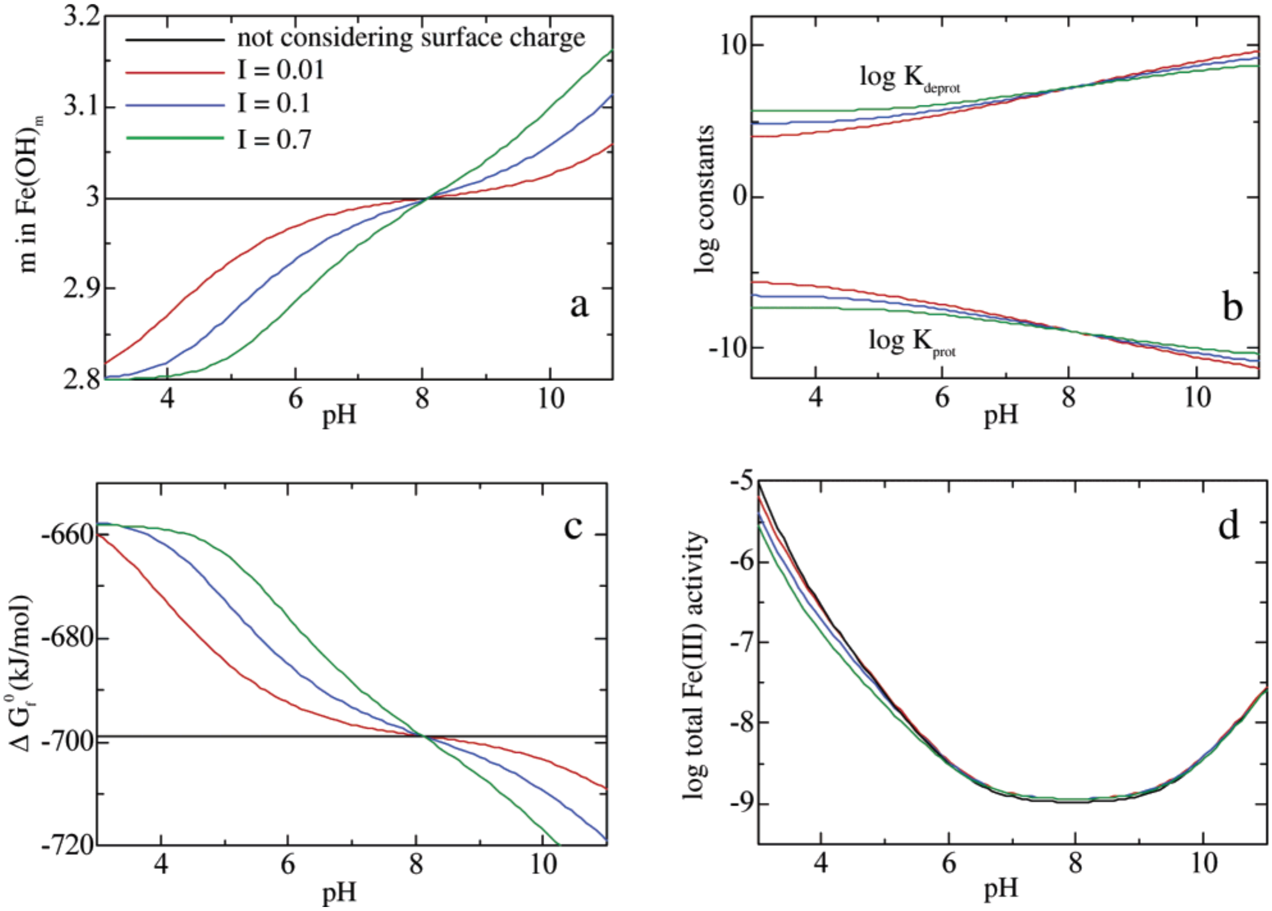

FIGURE 2. Change in *m* in Fe(OH)$_m$ as a function of pH and ionic strength (a). Changes in total protonation and deprotonation constants as a function of pH and ionic strength (b). Changes in ΔG_f^0 of charged HFO as a function of pH and ionic strength (c). Changes in total Fe(III) activity (total activity of all free and complexed Fe(III) in solution) as a function of pH and ionic strength of charged HFO as a function of ionic strength (d).

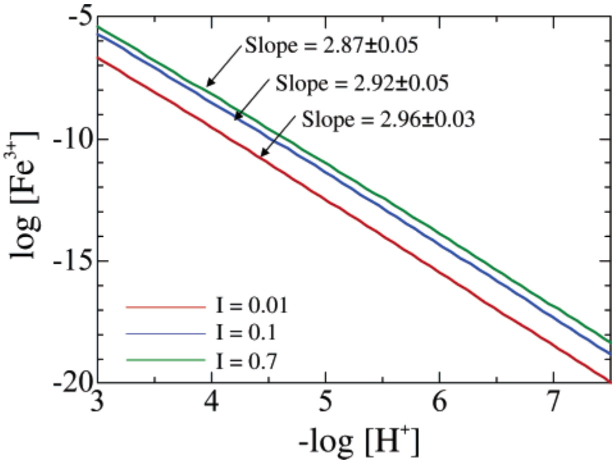

FIGURE 3. Calculated relationships between log[Fe^{3+}] and $-$log[H$^+$] at 25 °C under *I* = 0.01, 0.1, and 0.7.

The corresponding solubility constant for dissolution of charged HFO is calculated as

$$\log K_{\mathrm{dis}} = -\Delta G_{\mathrm{R}}^{\mathrm{dis}}/2.303RT \qquad (16)$$

Figure 2d shows the changes in total Fe(III) activity (total activity of all free and complexed Fe(III) in solution) as a function of pH and ionic strength calculated by using the hydrolysis constants of Fe(III) (hereafter solubility curve). The solubility curves for charged HFO indicated that surface charging resulted in a marked decrease in solubility under acidic conditions. Moreover, solubility decreased with increasing ionic strength under acidic conditions.

To compare with the previous observation (Figure 1), we calculated the log[Fe^{3+}] as a function of within the $-$log[H$^+$] range 3$-$7 under $I = 0.7$ as well as 0.01 and 0.1 (Figure 3). The log[Fe^{3+}] increases with the increase of ionic strength. It is due to the increase of activity coefficient with ionic strength. Although the calculated lines in Figure 3 appear to be linear, they actually are not. However, linear regression of the relationship between log[Fe^{3+}] and $-$log[H$^+$] under I = 0.7 gives a slope of 2.87 ± 0.05, a value less than 3, as observed previously. The slope increases with decrease of ionic strength. In an $I = 0.01$ system, the slope is nearly 3. The dependency on ionic strength is due to the enhancement of surface charging at higher ionic strength that leads to the significant change in stability of HFO. Although the slope under $I = 0.7$ is comparable to Figure 1, the calculated [Fe^{3+}] at a given $-$log[H$^+$] is 1 order of magnitude higher than that in Figure 1. This disagreement would be attributed to the value of free energy of formation of HFO (ΔG_f^0(HFO)) used in the calculation. We used the value from Stumm and Morgan (*14*) without any modification. However, the value is known to have large variation (*14*). It should be noted that the value of ΔG_f^0(Me(OH)$_3$) in eq 9 or eq 11 must be estimated from the "pure" Me(OH)$_3$, which does not charge or make surface complexes. We consider that the large variation in reported values of ΔG_f^0(HFO) is partly due to the fact that reported values of free energy of formation of HFO is not ΔG_f^0(Me(OH)$_3$) but ΔG_f^0(Me(OH)$_{3-x+y}^{x-y}$). The dotted red line in Figure 1 shows the results of calculation assuming ΔG_f^0-

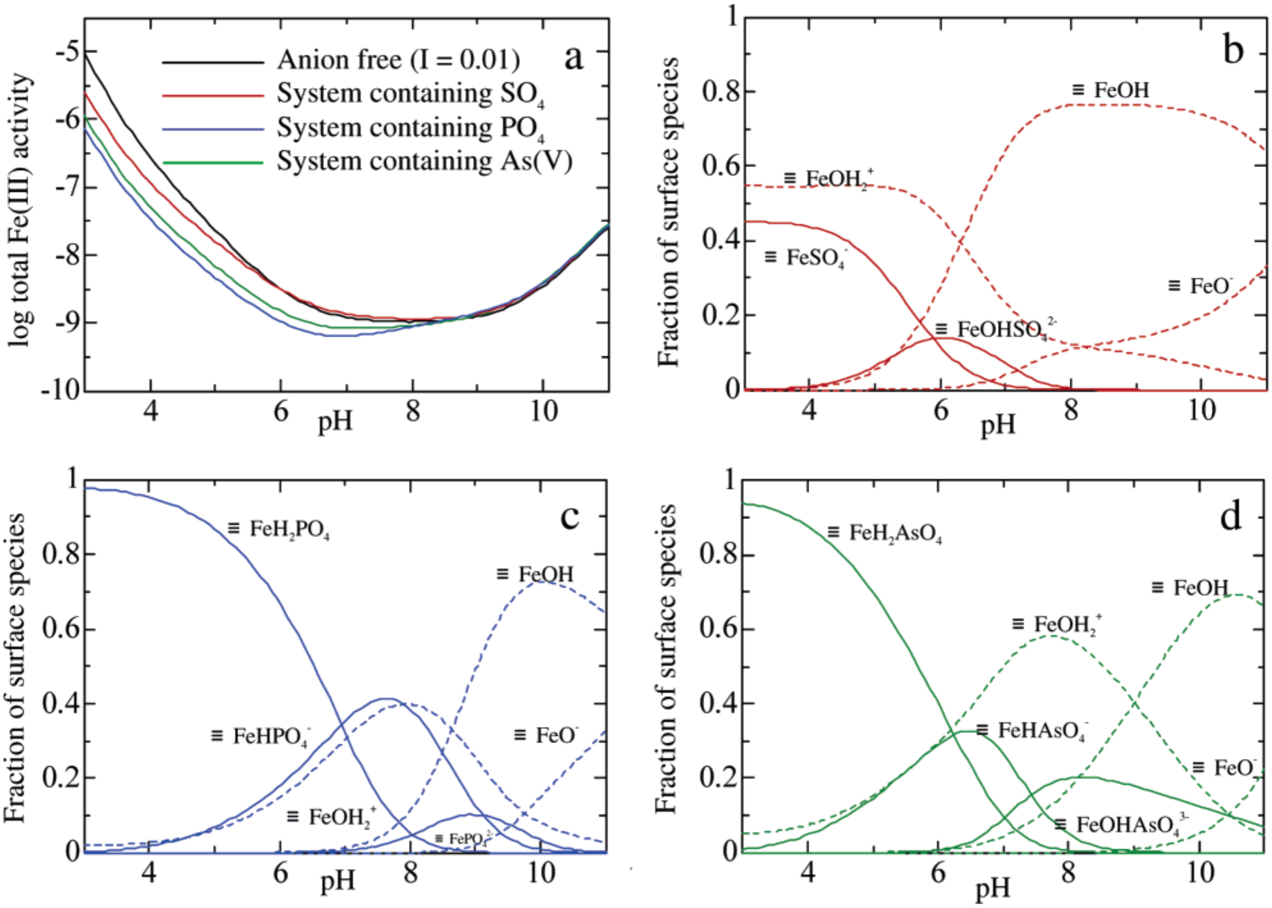

FIGURE 4. Solubility curves for surface-complexed HFO (a). Surface speciations of SO_4-containing (b), PO_4-containing (c), and As(V)-containing (d) systems (total concentration of each anion is 1 mM).

(HFO) = −693 kJ/mol. The line reproduces their experiments very well. This value of ΔG_f^0(HFO) represents the free energy of formation of "pure" HFO in the experiments by Byrne and Luo (*6*).

Effect of Anion Sorption. The solubility of ions coordinated to HFO can also be estimated if the surface complexation constants of the ions sorbed by HFO are available. Figure 4a shows the solubility curves for anion-free (considering only surface protonation and deprotonation) and SO_4, PO_4, and As(V) coordinated to HFO as a function of pH. The total concentrations of each anion were 1 mM. The solid concentration is 1 mmol $(Fe(OH)_3)$ L^{-1}. The ionic strength in each system was 0.01 M in the calculations. In all cases, anion sorption led to changes of Fe solubility relative to anion-free system, especially under neutral to acidic conditions. This result is due to preferential sorption of anions under neutral to acidic conditions (*2*). Figure 4b, which shows the surface speciation of SO_4 in the same system, indicates that, under acidic conditions, the fraction of SO_4 surface complexes becomes significant and the Fe solubility decreases markedly. In the systems containing PO_4 and As(V), the Fe solubility decreases at neutral to acidic pH. The magnitude of the decrease in Fe solubility for PO_4- and As(V)-coordinated HFO is greater than that for SO_4-coordinated HFO. The order of decrease is apparently consistent with the fraction of anion surface coverage (Figure 4b−d). Fukushi et al. (*2*) showed that the iron solubility of schwertmannite that sorbed As(V) is much lower than pure schwertmannite of which surface is occupied by SO_4. Paige et al. (*15*) showed that the iron solubility of HFO become much lower by sorption of As(V). Moreover, both field studies and laboratory studies have shown that sorption of PO_4 and As(V) leads to the inhibition of the transformation of HFO to more stable phases (*11*, *16*). The stabilization of HFO by sorption of As(V) and PO_4 demonstrated in our modeling would explain the results of the field and laboratory studies.

TABLE 4. As(V) Coordiantion Constants Estimated by Grossi et al. (*18*)

reaction	log *K*
$\equiv FeOH + AsO_4^{3-} + 3H^+ = \equiv FeH_2AsO_4 + H_2O$	30.6
$\equiv FeOH + AsO_4^{3-} + 2H^+ = \equiv FeHAsO_4^- + H_2O$	25.7
$\equiv FeOH + AsO_4^{3-} + H^+ = \equiv FeAsO_4^{2-} + H_2O$	21.2
$2 \equiv FeOH + AsO_4^{3-} + 3H^+ = \equiv Fe_2HAsO_4 + 2H_2O$	37.6
$2 \equiv FeOH + AsO_4^{3-} + 2H^+ = \equiv Fe_2AsO_4^- + 2H_2O$	32.0

All surface reactions in the FeOH.dat database are monodentate surface complexations (Table 1). However, numerous spectroscopic studies on anion sorption by HFO have indicated that several anions sorb to HFO via not only monodentate surface complexes but also bidentate surface complexes (e.g., ref *17*). To exemplify the effect of bidentate surface complexation on the stability of HFO, we calculated solubility curves for As(V)-coordinated HFO by using surface reactions estimated by Grossl et al. (*18*). Grossl et al. (*18*) used the iron oxide goethite as a sorbent and As(V) as a sorbate for their sorption experiments and employed a constant capacitance model to estimate a series of constants for bidentate surface complexation (Table 4). To test the applicability of their constants to our system (sorbent: HFO, electrostatic model: diffuse layer model), we compare the sorption behavior. The blue and red lines in Figure 5a represents the amount of As(V) sorption as a function of pH calculated by using the surface complexation constants of Grossl et al. (*18*) and FeOH.dat, respectively. The total

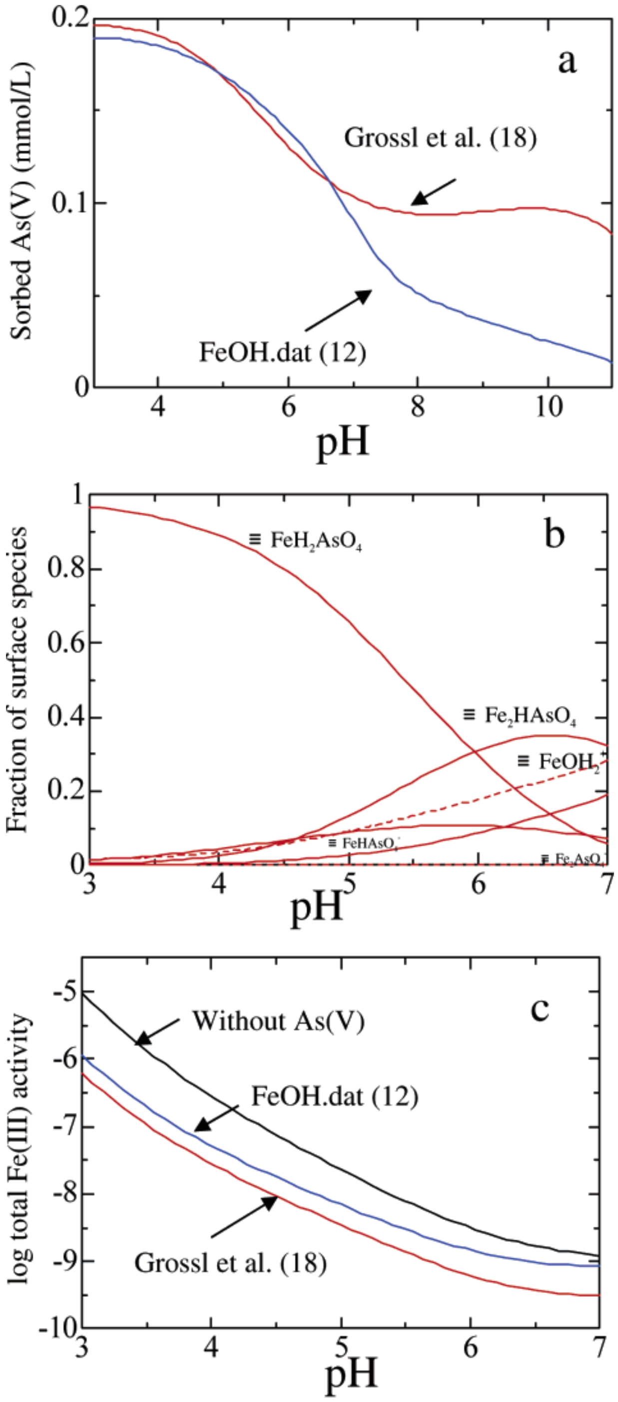

FIGURE 5. Comparison of amounts of As(V) sorption. "FeOH.dat (12)" denotes the calculation based on only monodentate coordination. "Grossl et al. (18)" is based on monodentate and bidentate coodination. Surface speciation of As(V) calculated by using the constants determined by Grossl et al. (*18*) (b). Solubility curves for As(V)-coordinated HFO. (c).

concentration of each anion was 1 mM in the calculations. The solid concentration is 1 mmol L^{-1}. The ionic strength in each system was 0.01 M. As shown in Figure 5a, the amount of As(V) sorption calculated by using Grossl et al. (*18*) is comparable to that by using FeOH.dat under the condition of pH 3−7. Therefore, the usage of the estimated constants by Glossl et al. (*18*) would be justified under the condition for the purpose of the exemplification of effect of bidentate coordination. Figure 5b shows the distribution of surface species as a function of pH. The bidentate surface complexes ($\equiv Fe_2HAsO_4$) become dominant at the condition of pH > 5. Concurrently, the solubility in this pH region significantly decreases (Figure 5c). The degree of decreasing solubility is greater than in the case only considering monodentate coordination (FeOH.dat) (see Figure 4d and compare the lines marked by arrows in Figure 5c). The bidentate complex is known to be a stronger bonding form than the monodentate complex, which would make the HFO more stable. The results of our modeling strongly indicate that the mechanistic understanding of the surface complexation is needed for the accurate prediction of the stability of nanoparticles.

The sorption process strongly influences the nature of nanoparticles. Nanoparticles are thought to be a labile phase, and the existence of this phase cannot influence the thermodynamically stable mineralogy and resultant solution chemistry. However, the change in stability resulting from the sorption process presumably changes the vector of the chemical evolution for both mineralogy and solution chemistry and may alter the equilibrium state that is predicted without considering the sorption process. This study also showed that geochemical modeling leads to the erroneous prediction of a natural system if the effect of the sorption process is not taken into account.

Acknowledgments

The manuscript benefited from the comments of four anonymous reviewers. Part of this study was supported by a grant from the 21st-Century COE (Center of Excellence) Program of the Japanese Ministry of Education, Culture, Science and Technology to T.S.

Literature Cited

(1) Banfield, J. F.; Zhang, H. Nanoparticles in the environment. In *Nanocrystals and the Environment*; Banfield, J. F., Navrotsky, A., Eds.; Reviews in Mineralogy and Geochemistry; Geochemical Society and Mineralogical Society of America: Washington DC, 2001; pp 1−59.

(2) Fukushi, K.; Sato, T.; Yanase, N. Solid-solution reactions in As(V) sorption on schwertmannite. *Environ. Sci. Technol.* **2003**, *37*, 3511−3516.

(3) Majzlan, J.; Navrotsky, A.; Schwertmann, U. Thermodynamics of iron oxides: Part III. Enthalpies of formation and stability of ferrihydrite (~$Fe(OH)_3$), schwertmannite (~$FeO(OH)_{3/4}(SO_4)_{1/8}$), and ϵ-Fe_2O_3. *Geochim. Cosmochim. Acta* **2004**, *68*, 1049−1059.

(4) Biedermann, G.; Chow, J. T. Studies on the hydrolysis of metal ions. Part 57. The hydrolysis of iron(III) ion and the solubility product of $Fe(OH)_{2.70}C_{0.30}$ in 0.5 M $(Na^+)Cl^-$ medium. *Acta Chem. Scand.* **1966**, *20*, 1376−1388.

(5) Fox, L. E. The solubility of ferric hydroxide and its relevance to iron concentrations in river water. *Geochim. Cosmochim. Acta* **1988**, *51*, 771−777.

(6) Byrne, H. B.; Luo, Y.-R. Direct observations of nonintegral hydrous ferric oxide solubility products: $K^*_{s0} = [Fe^{3+}][H^+]^{-2.86}$. *Geochim. Cosmochim. Acta* **2000**, *64*, 1873−1877.

(7) Dzombak, D. A.; Morel, F. M. M. *Surface Complexation Modeling—Hydrous Ferric Oxide*; Wiley-Interscience: New York, 1990.

(8) Davis, J. A.; Kent, D. B. Surface complexation modeling in aqueous geochemistry. In *Mineral−Water Interface Geochemistry;* Hochella, M. F., White, A. F., Eds.; Reviews in Mineralogy 20; Mineralogical Society of America: Washington, DC, 1990; pp 177−260.

(9) Stumm, W. *Chemistry of the Solid-Water Interface*; Wiley-Interscience: New York, 1992.

(10) Fukushi, K.; Sato, T.; Yanase, N.; Minato, J.; Yamada, H. Arsenate sorption on schwertmannite. *Am. Mineral.* **2004**, *89*, 1728−1734.

(11) Cornell, R. M.; Schwertmann, U. *The Iron Oxides*: *Structure, Properties, Reactions, Occurrences and Uses*: VCH: Weinheim, 1996.

(12) Bethke, C. M. *The Geochemist's Workbench Users Guide*; University of Illinois: 1998.

(13) Criscenti, L. J.; Sverjensky, D. A. The role of electrolyte anions ClO_4^-, NO_3^-, and Cl^- in divalent metal (M^{2+}) adsorption on oxide and hydroxide surfaces in salt solutions. *Am. J. Sci.* **1999**, *299*, 828−899.

(14) Stumm, W.; Morgan, J. J. *Aquatic Chemistry*, 3rd ed.; Wiley-Interscience: New York, 1996.

(15) Paige, C. R.; Snodgrass, W. J.; Nicholson, R. V.; Scharer, M. An arsenate effect on ferrihydrite dissolution kinetics under acidic oxic conditions. *Water Res.* **1997**, *31*, 2370−2382.

(16) Cornell, R. M.; Giovanoli, R.; Schneider, W. Review of hydrolysis of iron(III) and the crystallization of amorphous iron(III) hydroxide hydrate. *J. Chem. Technol. Biotechnol.* **1989**, *46*, 115−134.

(17) Waychunas, G. A.; Rea, B. A.; Fuller, C. C.; Davis, J. A. Surface chemistry of ferrihydrite: Part 1. EXAFS studies of the geometry of coprecipitated and adsorbed arsenate. *Geochim. Cosmochim. Acta* **1993**, *57*, 2251−2270.

(18) Grossl, P. R.; Eick, M.; Sparks, D. L.; Goldberg, S.; Ainsworth C. C. Arsenate and chromate retention mechanisms on goethite. 2. Kinetic evaluation using a pressure-jump relaxation technique. *Environ. Sci. Technol.* **1997**, *31*, 321−326.

Received for review May 30, 2004. Revised manuscript received October 7, 2004. Accepted November 1, 2004.

ES0491984